Available online at www.sciencedirect.com
SCIENCE DIRECT®
Biochimica et Biophysica Acta 1611 (2003) 140–150
BIOCHIMICA ET BIOPHYSICA ACTA
BBA
www.bba-direct.com

Cytosolic delivery of macromolecules: I. Synthesis and characterization of pH-sensitive acyloxyalkylimidazoles

Feng-Jing Chen[a], Aravind Asokan[b], Moo J. Cho[b,*]

[a] *Lipocine Inc., Salt Lake City, UT 84103, USA*
[b] *Division of Drug Delivery and Disposition, CB # 7360, School of Pharmacy, University of North Carolina at Chapel Hill, Chapel Hill, NC 27599-7360, USA*

Received 2 October 2002; received in revised form 16 January 2003; accepted 24 January 2003

Abstract

A series of 1-(acyloxyalkyl)imidazoles (AAI) were synthesized by nucleophilic substitution of chloroalkyl esters of fatty acids with imidazole. The former was prepared from fatty acid chloride and an aldehyde. When incorporated into liposomes, these lipids show an apparent pK_a value ranging from 5.12 for 1-(palmitoyloxymethyl)imidazole (PMI) to 5.29 for 1-[(α-myristoyloxy)ethyl]imidazole (α-MEI) as determined by a fluorescence assay. When the imidazole moiety was protonated, the lipids were surface-active, as demonstrated by hemolytic activity towards red blood cells. As expected, AAI were hydrolyzed in serum as well as in cell homogenate. They were significantly less toxic than biochemically stable *N*-dodecylimidazole (NDI) towards Chinese hamster ovary (CHO) and RAW 264.7 (RAW) cells as determined by MTT assay. When fed to RAW cells, fluorescein-labeled oligonucleotides encapsulated in liposomes containing 20 mol% 1-(stearoyloxymethyl)imidazole (SMI) resulted in punctate as well as partially diffuse fluorescence. In a functional assay involving down-regulation of luciferase in CV-1 cells, neutral liposomes containing imidazole lipids showed suboptimal delivery of antisense phosphorothioate oligomers. Taken together, the results suggest that AAI are of potential use in developing nontoxic, pH-sensitive liposomes. However, these liposomal formulations need to be optimized to achieve higher concentrations of pH-sensitive detergents within the endosome to facilitate efficient cytosolic release of liposome-entrapped contents.

Keywords: Cytosolic delivery; Macromolecule; Synthesis

1. Introduction

Membrane-impermeable macromolecules enter the eukaryotic cell primarily via endocytosis [1]. Acidification associated with endosome maturation has been exploited in the design of pH-sensitive drug carriers for cytosolic delivery of therapeutic agents [2,3 and references therein]. For instance, liposomal formulations containing dioleoyl phosphatidylethanolamine (DOPE), oleic acid, cholesteryl hemisuccinate or imidazole-based amphiphiles have shown efficient cellular delivery of encapsulated macromolecules [4–6]. While net surface charge in such formulations can facilitate liposome–cell interactions and enhance cellular uptake [7,8], it tends to promote nonspecific interactions with serum proteins causing rapid clearance from the circulation [9,10]. Our research objective has been to develop neutral liposomal formulations, which can be triggered by acidic endosomal pH to release entrapped contents to cytosol.

An imidazole (pK_a = 6.9) or morpholine (pK_a = 8.4) derivative containing a long alkyl chain, commonly referred to as lysosomotropic detergents [11], becomes surface-active when the nitrogen is protonated in the endosome. For instance, cytotoxicity of *N*-dodecylimidazole (NDI) was originally attributed to the leakage of lysosomal enzymes into the cytosol [12]. Although the above interpretation was disputed in subsequent studies, a consensus is that the persistent cytotoxicity clearly originates from two sources: surface activity and biochemical stability of the lysosomotropic detergent [13–15].

In an attempt to reduce this cytotoxicity, while maintaining the surface activity, we have developed a series of biodegradable and thus 'soft' lysosomotropic 1-(acyloxyalkyl)imidazole (AAI) detergents (Table 1). A similar biodegradable, pH-sensitive surfactant, dodecyl-2-(1′-imida-

* Corresponding author. Tel.: +1-919-966-1345; fax: +1-919-966-7778.
E-mail address: m_j_cho@unc.edu (M.J. Cho).

0005-2736/03/$ - see front matter © 2003 Elsevier Science B.V. All rights reserved.
doi:10.1016/S0005-2736(03)00049-X

Table 1
Structures and pK_a values of AAI and other weak base lipids

Chemical name (Abbreviation)	Structure	pKa
1–[(α–Myristoyloxy)ethyl]imidazole (α–MEI)	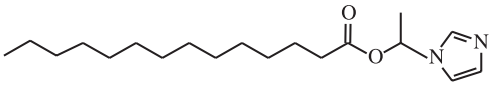	5.29
1-(Myristoyloxymethyl)imidazole (MMI)	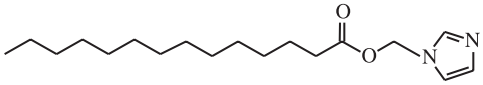	5.18
1-(Palmitoyloxymethyl)imidazole (PMI)	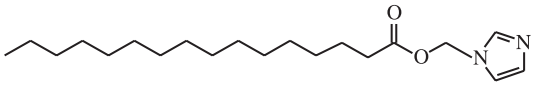	5.12
1-(Stearoyloxymethyl)imidazole (SMI)	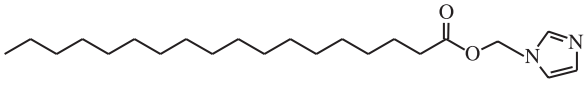	5.17
1-(Oleoyloxymethyl)imidazole (OMI)	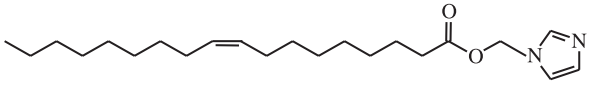	5.18
1-(Linoleoylmethyl)imidazole (LMI)	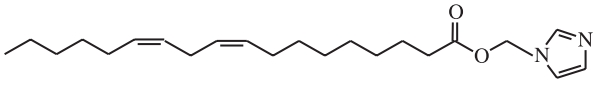	5.14
N-Tetradecylimidazole (NTI)	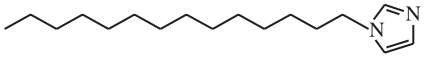	6.33
N-Dodecylimidazole (NDI)	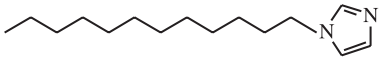	6.3 [a]
Dodecyl-2-(1'-imidazolyl)propionate (DIP)	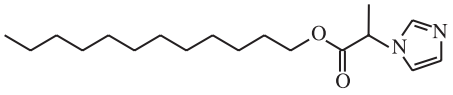	6.8 [b]
N-Dodecylmorpholine (NDM)	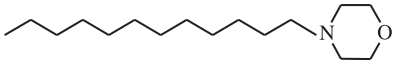	7.6 [a]

[a] The pK_a values of NDI and NDM were obtained from Ref. [14].
[b] The pK_a value of DIP was obtained from Ref. [16].

zolyl) propionate (DIP), has been reported in the literature [16]. While DIP is expected to degrade into imidazolyl propionic acid and dodecyl alcohol, AAI are hydrolyzed enzymatically to fatty acid and unstable hydroxymethyl imidazole. The latter spontaneously releases an aldehyde and an imidazole. In short, AAI were expected to maintain their lysosomotropic detergency and biochemical lability. In addition, these fatty acid derivatives should spontaneously insert themselves into liposomal bilayers at a wide range of concentrations, where they would predominantly exist as unprotonated species at neutral pH. As phagocytosis by the target cell proceeds, the liposomes would encounter an acidic endosomal environment [17]. From this point on, a cascade of events should occur as shown in Fig. 1.

As endosomal pH drops, the imidazole moiety will be protonated with a diffuse positive charge between the *N*1 and *N*3 positions. The increase in hydration associated with protonation is expected to induce membrane defects and significant leakage of the entrapped macromolecules. In addition, upon protonation, AAI would become surface-active, creating transient defects or pores in the endosomal membrane that would eventually allow mass transfer into the cytosol [18,19]. The structure–activity relationship in this context constitutes the crux of the present in vitro study.

2. Materials and methods

2.1. Lipids and chemicals

N-Tetradecylimidazole (NTI) and the following AAI were provided by Megabios Corp. (Burlingame, CA): 1-(palmitoyloxymethyl)imidazole (PMI), 1-(stearoyloxymethyl)imidazole (SMI), 1-(oleoyloxymethyl)imidazole (OMI), and 1-(linoleoyloxymethyl)imidazole (LMI). Egg phosphatidylcholine (EPC), dipalmitoyl phosphatidylcholine (DPPC), and DOPE were obtained from Avanti Polar Lipids, Inc. (Alabaster, AL). Myristoyl chloride, paraldehyde, (3-[4,5 -yl]-2,5-diphenyltetrazolium bromide (MTT), potassium 2-(*p*-toluidino) naphthalene-6-sulfonate (TNS), nigericin, calcein, and cholesterol were purchased from Sigma Chemical Co. (St. Louis, MO). Culture medium, fetal bovine serum (FBS), antibiotics, and supplements were obtained from Gibco BRL (Grand Island, NY). All other

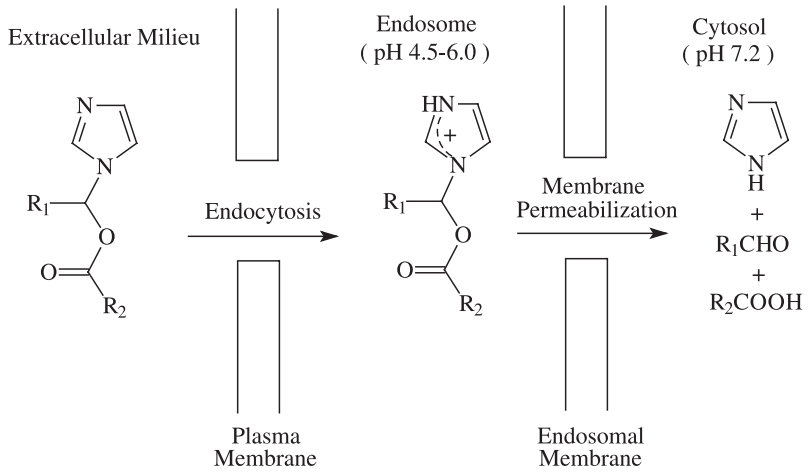

Fig. 1. Rationale and proposed mechanism of cytosolic delivery mediated by AAI. Upon incorporation into liposomes, AAI are endocytosed into target cells. In the acidic endosomal milieu, the imidazole lipids acquire surface activity, which results in sequential permeabilization of both the liposomes and endosomes, thus allowing entrapped drug molecules to escape to the cytosol of cells. To reduce cytotoxicity, AAI are designed to be biodegradable. Following enzymatic hydrolysis of the ester bond, the resulting hydroxymethyl imidazoles are expected to rapidly breakdown into imidazole and the corresponding aldehyde.

chemicals or reagents were obtained from Aldrich Chemical (Milwaukee, WI). Unless mentioned otherwise, all materials were used as received without any further purification.

2.2. Synthesis

1-(Myristoyloxymethyl)imidazole (MMI) and 1-[(α-myristoyloxy)ethyl]imidazole (α-MEI) were prepared according to Bodor [20]. Typical synthetic procedure is illustrated for MMI: 1 ml (3.57 mmol) of myristoyl chloride and 113 mg (3.57 mmol) of paraformaldehyde were heat-sealed in an ampule and maintained at 95 °C for 3 days. The reaction mixture was diluted in hexane then chromatographed on silica gel eluting with hexane/EtOAc (98:2, v/v), then on Florisil®, eluting with hexane followed by hexane/EtOAc (98:2, v/v). Approximately 945 mg of chloromethyl myristate was obtained and the yield of this reaction was ~ 31%. The purity of the product was examined by silica gel TLC which showed only one spot: R_f = 0.50 [hexane/EtOAc (95:5, v/v)]. ^{1}H NMR ($CDCl_3$): δ 5.7 (s, 2H), 2.4 (t, 2H), 1.6–1.7 (m, 2H), 1.3 (br s, 20H), 0.9 (t, 3H). To a solution of 915 mg (3.30 mmol) of chloromethyl myristate in 20 ml of CH_3CN, 270 mg (3.97 mmol) of imidazole was added and refluxed at 82 °C for 12 h. The solvent was removed and methylene chloride half saturated with a 28% ammonium hydroxide aqueous solution was added to neutralize the HCl generated from the reaction. The clear filtrate of the reaction mixture in CH_2Cl_2 was concentrated and chromatographed on silica gel eluting with CH_2Cl_2/EtOAc/MeOH (90:8:2, v/v).

Approximately 625 mg of the free base of MMI was obtained and was subsequently converted to HCl salt. The free base (300 mg) dissolved in 15 ml of anhydrous diethyl ether was bubbled with anhydrous HCl gas. The HCl salt of MMI precipitated out from the ether immediately was collected by filtration through a medium-porosity sintered glass. Approximately 260 mg of MMI·HCl was obtained after drying the precipitate under vacuum overnight and the yield of this reaction was about 47.6%. The purity of the product was examined by silica gel TLC, which showed only one spot: R_f = 0.31 [CH_2Cl_2/EtOAc/MeOH (80:18:2, v/v)], m.p. 112–114 °C. ^{1}H NMR ($CDCl_3$): δ 9.8 (s, 1H), 7.4 (d, 2H), 6.3 (s, 2H), 2.4 (t, 3H), 1.6 (br m, 2H), 1.2–1.3 (br s, 20H), 0.9 (t, 3H). FAB-MS: *m/z* 309.2 ($M+H^+$). Anal. calculated for $C_{18}H_{33}N_2O_2Cl$: C, 62.68, H, 9.64, N, 8.12, Cl, 10.28. Found: C, 62.55, H, 9.70, N, 8.10, Cl, 10.28. In all instances, the NMR spectra were recorded on a Bruker AC-300 spectrometer; FAB-MS spectra were obtained from a VG-70-250 SEQ mass spectrometer; and elemental analysis performed by Atlantic Microlab (Norcross, GA).

For the HCl salt of α-MEI HCl, R_f = 0.35 [CH_2Cl_2/EtOAc/MeOH (80:18:2, v/v)], m.p. 74–76 °C. ^{1}H NMR ($CDCl_3$): δ 9.4 (s, 1H), 7.4 (d, 2H), 6.9 (q, 2H), 2.4 (br m, 3H), 1.9 (d, 2H), 1.6 (br m, 2H), 1.25 (br s, 20H), 0.9 (t, 3H). FAB-MS: *m/z* 323.2 ($M+H^+$). Anal. calculated for $C_{19}H_{35}N_2O_2Cl$: C, 63.58, H, 9.83, N, 7.80, Cl, 9.88. Found: C, 63.37, H, 9.80, N, 7.83, Cl, 9.94.

2.3. Preparation of liposomes

For pK_a measurement and cytotoxicity study of AAI, blank liposomes were prepared by freeze-thaw and extrusion method [21]. Briefly, EPC, cholesterol, and AAI (45:45:10 in molar ratio), dissolved in chloroform/ethanol mixture, were evaporated in vacuo to form lipid films. After drying overnight under high vacuum, dry lipid films were hydrated with phosphate buffered saline (PBS) by vortexing. The resulting multilamellar vesicles were freeze-thawed in a dry ice/acetone bath and lukewarm water bath for six cycles. The liposomes were extruded through two stacked 0.1 μM polycarbonate membranes (Poretics, Livermore, CA) by nitrogen at room temperature for 10 times with an extruder (Lipex Biomembranes, Vancouver, Canada).

Liposomes containing antisense phosphorothioate oligonucleotides (S-ODN) or fluorescein conjugated phosphorothioate oligonucleotides (F-ODN) were prepared by freeze-thaw and extrusion along with the minimum volume entrapment method for high entrapment of oligonucleotides. Briefly, dry lipid films of AAI and other natural occurring lipids were hydrated in 40–60 μl of distilled water containing 30–90 nmol of F-ODN by alternatively vortexing and storing at 4 °C overnight. The lipid suspensions were then diluted in 1 ml of PBS and freeze-thawed. The resulting vesicles were extruded through two stacked 0.1-μm polycarbonate membranes 12 times by N_2 head pressure. Unentrapped F-ODN was removed by spin column gel permeation chromatography on Sepharose CL-6B in a 20-ml syringe and eluted with PBS [22]. In all cases, less than 3 ml of the liposome preparation was applied to the gel bed. The column was spun at $40 \times g$ for 5 min at 4 °C to facilitate elution of the oligonucleotide-containing liposomes. Free F-ODN retained by Sepharose beads was recovered by washing the column.

The S-ODN concentrations in liposome preparations were determined by capillary electrophoresis. Briefly, a 200-μl aliquot of the liposome fraction was dissolved in 400 μl of isopropanol and all the solvents were removed subsequently. The residue was reconstituted in 400 μl of deionized water and the suspension was centrifuged at $16{,}000 \times g$ for 20 min. The clear supernatant was withdrawn and S-ODN analyzed in a Beckman P/ACE System 2000 (Fullerton, CA) equipped with a capillary (50 cm × 75 μm cartridge). The capillary was then eluted with 100 mM sodium borate at pH 8.35, driven by a voltage of 30 kV at 23 °C. Appearance of S-ODN was monitored by a UV detector at 214 nm. Entrapment of S-ODN was also estimated by subtracting the amount of unencapsulated S-ODN obtained based on the UV absorbance of liposome-free fractions at 260 nm. The F-ODN concentration of the liposome preparations was determined by a fluorescence assay on a Perkin Elmer LS-50B spectrofluorometer (Norwalk, CT) with $\lambda_{ex} = 485$ nm and $\lambda_{em} = 516$ nm. Entrapped F-ODN was released by adding 200 μl of 1% triton X-100 solution to 100 μl of liposome preparation, and then diluted to 2 ml in deionized water. Size distribution of the liposomes was determined by photon correlation spectroscopy using a NICOMP 370 submicron particle sizer (Particle Sizing Systems, Santa Barbara, CA). The osmolality of liposome preparations was determined by means of freezing-point depression measurement on a Fiske ONE-TEN Osmometer (Fiske Associates, Norwood, MA).

2.4. Determination of pK_a of AAI in liposomes

Blank unilamellar vesicles containing AAI, EPC, and cholesterol were diluted to 60 μM of total lipid in 150 mM NaCl, 5 mM HEPES, 5 mM ammonium acetate, 20μM TNS, and 0.1 μM nigericin at pH ranging from 2 to 10. The surface charge of liposomes at each pH was monitored by determining the TNS fluorescence in a Perkin Elmer LS-50B spectrofluorometer using $\lambda_{ex} = 332$ nm and $\lambda_{em} = 440$ nm [23]. Data were subjected to least square analysis (MINSQ program) using the following equation to obtain values of pK_a, where A and B are constants.

$$\text{Fluorescence} = A + \frac{B \times K_a}{K_a + [H^+]}$$

2.5. pH-dependent surface activity of AAI

Human erythrocytes were suspended in 50 ml of buffers at 2.5×10^7 cells/ml with a pH range of 5.0 to 7.5 at 37 °C under constant hydrodynamic conditions. A stock solution of MMI in ethanol was added to the suspended erythrocytes to a final concentration 0.05 mM with 2% of ethanol. At each time point, 1 ml of the suspension was withdrawn and centrifuged at $2000 \times g$ for 1 min at room temperature. The absorbance of the clear supernatant at 533 nm was measured in a Shimadzu UV/Vis spectrophotometer (Kyoto, Japan). Complete hemolysis was determined by adding Triton X-100 to the suspended erythrocytes in the presence of 2% ethanol so that the final concentration was 0.01%. Negative controls were obtained by suspending the erythrocytes in buffers of pH ranging from 5.0 to 7.5 in the presence of 2% ethanol.

2.6. Cell culture and oligonucleotides

Chinese hamster ovary (CHO) and RAW 264.7 (RAW) cell lines were obtained from American Type Culture Collection (Rockville, MD). CV-1 cells expressing luciferase were a generous gift from Dr. C. Leamon formerly at Glaxo (Research Triangle Park, NC). All cells were maintained as plated at 37 °C in a humidified atmosphere of 5% CO_2, α-MEM supplemented with L-glutamine, antibiotics, and 10% heat-inactivated FBS for CHO cells; RAW cells in DMEM-H medium supplemented with L-glutamine, antibiotics, and 10% heat-inactivated FBS; and CV-1 cells in MEM supplemented with essential amino acids, sodium pyruvate, antibiotics, and 10% heat-inactivated FBS.

Antisense oligomers (S-ODN and 3′-labeled F-ODN) were prepared by the Nucleic Acid Core Facility in the Lineberger Cancer Research Center of UNC (Chapel Hill, NC). The oligonucleotide (5′-TGGCGTCTTCCATTT-3′) complementary to the initiation codon region of the luciferase mRNA of the CV-1 cells has been known to inhibit the translation of luciferase [24].

2.7. Biodegradability of AAI

Stability of AAI was determined at 37 °C in human serum (Sigma) and in CHO cell homogenate. The latter was prepared by homogenizing CHO cells in exponentially growing phase at 3×10^7 cell/ml in PBS on ice with a tissue homogenizer (Thomas Scientific, Swedesboro, NJ). Cell number was determined using a hemocytometer. The result-

ing cell homogenate was kept frozen at − 20 °C until further use.

Stock solutions of AAI prepared in ethanol were added to human serum or CHO cell homogenate at 37 °C in such a way that the initial concentration of AAI was 0.1 mM and ethanol concentration was 2% in all the samples. The samples were then incubated in a water bath maintained at 37 °C. At each time point, a 300-μl aliquot of the sample was withdrawn and mixed with 300 μl of cold acetonitrile by vortexing, then centrifuged at 16,000 × *g* for 7 min. The concentration of AAI remaining in the clear supernatant was determined by an HPLC assay. Human serum samples of PMI, OMI, and NTI were analyzed on a Econisil® C18 column (10 μm, 250 × 4.6 mm) (Alltech, Deerfield, IL) eluting with a mobile phase of 40% isopropanol, 40% methanol, and 20% pH 8, 0.05% (v/v) 3-amino-1-propanol aqueous solution at a flow rate of 1.5 ml/min. Human serum samples of other AAI and CHO cell homogenate samples were analyzed on a Econisil® C8 column (10 μm, 250 × 4.6 mm) (Alltech) eluting with a mobile phase of 40% isopropanol, 40% methanol, and 20% 25 mM Na_2PO_4 aqueous solution at pH 5, at a flow rate of 1.0 ml/min. The eluent was monitored by a Rainin Dynmax® model UV-C detector at 220 nm and recorded by a Shimadzu Chromatopac CR601 integrator.

2.8. Cytotoxicity of AAI

The cytotoxicity of AAI to CHO and RAW cells was evaluated by the MTT assay [25]. Briefly, AAI, either in ethanol or in liposomes, were diluted in culture media containing serum and incubated with cells in 96-well plates at a cell density of 2.5×10^4 for LC_{50} and at 1.25×10^4 cells for IG_{50} determination. In the former, the final ethanol concentration was 1% and the total lipid concentration was 10-fold higher than that used for the latter. Cells were incubated with AAI at 37 °C for 90 min for the determination of LC_{50} and 48 h for the determination of IG_{50}. At the end of incubation, MTT solution was added to each well, and plates were incubated for an additional 4 h. After aspirating the media, 0.05 N HCl in DMSO was added to dissolve the MTT formazan produced by the cells. The absorbance at 490 nm was read on a Bio-Rad plate reader (Hercules, CA) and used in calculating the cell viability according to the literature [25].

2.9. Intracellular distribution of F-ODN

CV-1 cells were grown on a coverslip inside the six-well plate at a seeding concentration of 4×10^5 cells/well. After 24 h of incubation, cells were incubated with F-ODN alone or liposomes containing F-ODN in culture medium with or without 10% FBS at 37 °C. The cells were then washed in PBS and fixed with 4% formaldehyde in PBS at 4 °C for 15 min. To preserve the specimen, cells were immersed in a 1:1 mixture of glycerol and PBS in the dark at 4 °C after removing the fixative by aspiration. The cells were later examined using a Zeiss Axiovert 100 TV fluorescence microscope excited at 488 nm.

2.10. Antisense activity of S-ODN facilitated by AAI

Luciferase-expressing CV-1 cells were seeded at 2×10^5 cells in each well of six-well plates. After 24 h of incubation, cells were incubated with S-ODN alone or liposomes entrapping S-ODN in culture medium with or without 10% whole FBS for 4 h at 37 °C. The liposomes were removed by aspiration, replaced with media containing 10% heat-inactivated FBS, and incubated for another 20 h. At the end of incubation, cells were immediately processed for determining the level of luciferase expression using the Enhanced Luciferase Assay Kit (Analytic Luminescence Laboratory, Ann Arbor, MI) on a Monolight 2010 luminometer. Cell viability based on total protein per well was determined by BCA protein assay (Pierce) on a Bio-Rad model 3550 microplate recorder. Luciferase inhibition was obtained by normalizing the relative luminescent unit (RLU) against the total protein and compared with the negative control.

3. Results

3.1. pK_a of AAI in liposomes

The pH dependence of fluorescence intensity of TNS upon incorporation in liposomes containing AAI is shown in Fig. 2; and the pK_a of AAI and similar lipophilic weak bases summarized in Table 1. The pK_a value of NTI that we obtained, 6.33, is in good agreement with that of NDI, 6.3 [14]. As expected, the pK_a of AAI remains approximately the same (5.16 ± 0.03), despite structural differences in their fatty acid chains. The pK_a of α-MEI is about 0.13 units higher than the average pK_a of AAI. However, the pK_a values of all AAI are significantly lower (1.0–1.2 unit) than that of the plain tertiary amine NTI.

3.2. pH-dependent surface activity of AAI

AAI are practically insoluble in water even at a pH close to their pK_a, however, soluble at lower pH. Considering the potential hydrolysis of the ester bond at low pH, only the most stable α-MEI was subject to determination of the critical micellar concentration at pH 2.7: 1.5×10^{-4} M when measured by surface tension using a Krüss digital tensiometer (platinum–iridium ring) at 25 °C. The reduction in surface tension was about 40 dyne/cm (data not shown).

As shown in Fig. 3A, hemolysis of erythrocytes by MMI at neutral pH showed a lag time of 20 min, and 100% hemolysis was achieved 50 min after adding MMI. At pH 6.0, the onset time decreased to 10 min, and it took only about another 10 min to reach 100% hemolysis. Upon further decrease of pH to 5.5, the lag time was only about 2 min and

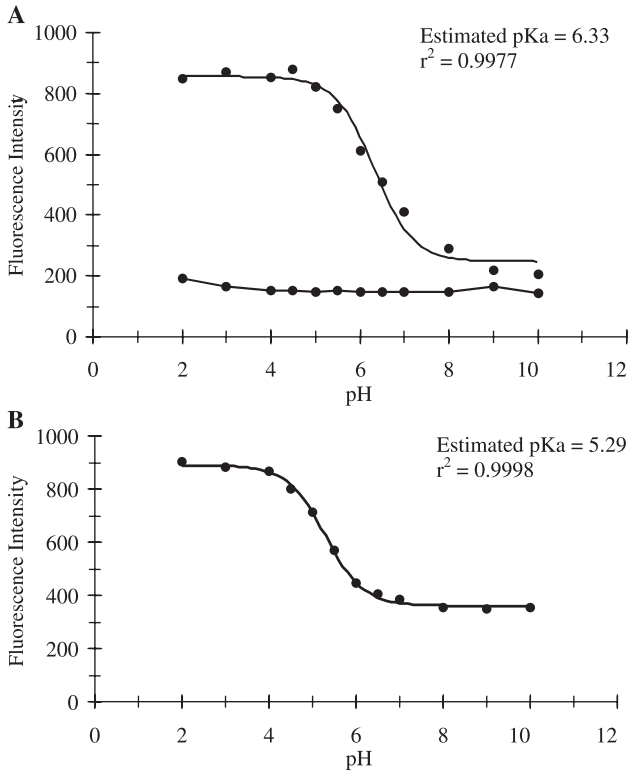

Fig. 2. pH-dependence of TNS fluorescence upon incorporation into EPC/cholesterol liposomes containing (A) 0% (lower plot) or 10% NTI (upper curve) and (B) α-MEI. The pK_a values were obtained by nonlinear regression analysis of the data.

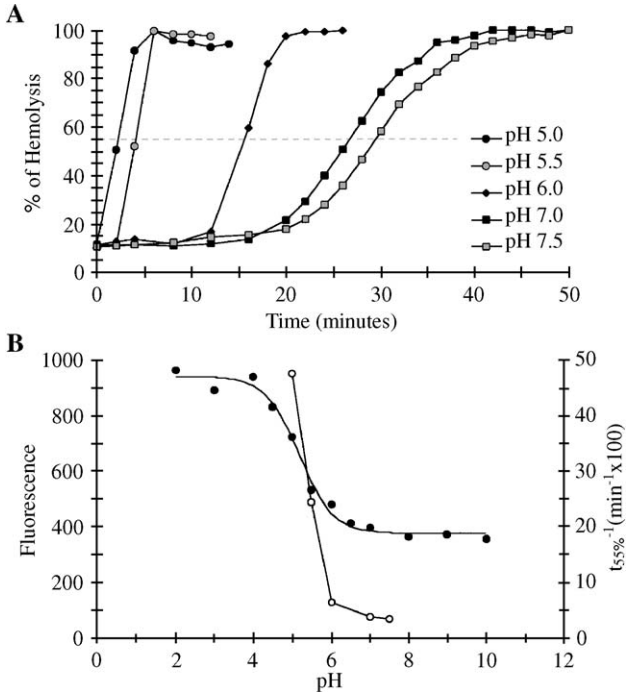

Fig. 3. pH-dependent hemolysis of human erythrocytes by MMI. (A) The time course of hemolysis by 0.05 mM MMI in erythrocyte suspensions (2.5×10^7/ml) at various pH in the presence of 2% ethanol at 37 °C under constant hydrodynamics. Complete (100%) hemolysis was obtained by adding triton X-100 to the erythrocyte suspension. (B) The correlation between the protonation of MMI and the effect of MMI on the hemolysis of erythrocytes was obtained by superimposing the titration curve of MMI (closed symbols) with the equivalent hemolysis rate caused by MMI (open symbols; obtained by taking the reciprocal of time required to achieve 55% of total hemolysis, dotted line).

hemolysis was complete within 6 min. Finally, at pH 5.0 or lower, the hemolysis occurred instantly upon adding MMI. A comparison of the pH-titration profile of MMI with the equivalent rate of hemolysis (reciprocal of time required to achieve 55% of total hemolysis) with respect to changes in pH is shown in Fig. 3B. At pH 6, one pH unit higher than the pK_a of MMI, protonation of as little as 10% MMI seems to be sufficient to induce the observed rapid increase in the hemolysis rate. When about 50% MMI was activated at pH 5.0, hemolysis appears to reach the maximum rate.

3.3. In vitro stability of AAI

The control compound NTI was stable in both human serum and CHO cell homogenate within the time frame of the experiment. In contrast, all AAI were found to degrade in human serum and CHO cell homogenate at 37 °C following a first-order kinetic process up to four half-lives (raw data not shown). The apparent first-order rate constants of decomposition of AAI in human serum (k_S) and in CHO cell homogenate (k_H) are summarized in Table 2. Interestingly, as shown in Fig. 4, the order of stability of AAI is the same both in human serum and CHO cell homogenate. The stability of AAI increased with the chain length of the saturated fatty acids, from C14 to C18. However, a dramatic decrease in the stability was observed as the C18 fatty acid becomes successively more unsaturated, from stearic to oleic to linoleic acid. In addition, substitution of the α-carbon in MMI with a methyl group made α-MEI much more stable in serum and cell homogenate.

The intrinsic octanol–water partition coefficients (log P) of AAI summarized in Table 2 were estimated using a computer program ACD/ILAB™ (Advanced Chemistry Development, Toronto, Ontario, Canada). When the k_S was plotted against the corresponding log P, a good linearity was observed for the three fully saturated AAI: MMI, PMI, and SMI (plots not shown). However, unsaturated C18 lipids

Table 2
Apparent first-order rate constants of the degradation of AAI in serum (k_S), CHO cell homogenate (k_H), their ratios and intrinsic octanol–water partition coefficients (the latter was estimated using a computer program ACD/ILAB™)

	$k_S \times 10^4$ (min^{-1})	$k_H \times 10^4$ (min^{-1})	k_H/k_S	log P
α-MEI	9.3	99.3	10.7	6.61
MMI	67.4	339.8	5.0	6.27
PMI	36.2	235.0	6.5	7.33
SMI	8.1	75.3	9.2	8.39
OMI	66.5	286.4	4.3	7.87
LMI	157.9	450.1	2.9	6.44

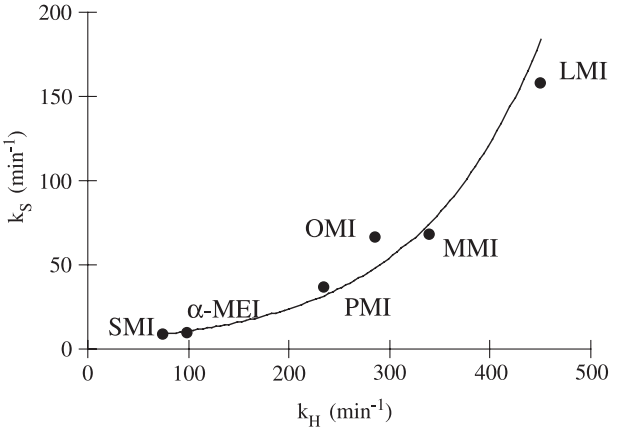

Fig. 4. A comparison of apparent first-order rate constants of degradation of AAI in human serum (k_S) and CHO cell homogenate (k_H, 3×10^7 cells/ml of PBS) at 37 °C.

(OMI and LMI) deviated positively from the straight line, while α-MEI showed negative deviation. Similar observations were also obtained when k_H was plotted against the corresponding log *P*. In addition, AAI were found to degrade more rapidly in CHO cell homogenate than in serum, supporting potential use in systemic applications in vivo.

3.4. Cytotoxicity of AAI

Biodegradable AAI were at least 10 times less cytotoxic than the nonbiodegradable control compound, NTI, whether they were given to cells in solution or incorporated into liposomes (shown in Table 3). In general, the concentrations of AAI required to kill 50% of the cells (LC_{50}) were at least 10 times higher than that required to inhibit 50% of the cell growth (IG_{50}). No significant difference in the cytotoxicity to CHO cells was observed whether imidazole lipids were given to cells in solution or incorporated into liposomes. However, there was significant difference in the cell growth inhibition (IG_{50}) by liposomal AAI in two different cell lines. Up to threefold increase in cytotoxicity is seen for the more phagocytic RAW cells after prolonged exposure (2 days) to AAI relative to CHO cells. An unexpected observation is that LMI and MMI incorporated into liposomes were most toxic to RAW cells in terms of the IG_{50} values. These lipids were 2–3 times more toxic than other AAI, even though they appeared to be 4–17 times more labile in human serum and CHO cell homogenate than α-MEI or SMI (based on the difference in k_S and k_H).

Table 3
Cytotoxicity of AAI and NTI on CHO and RAW cells by MTT assay[a]

Cell line	CHO				RAW	
Formulation	Solution	Liposome	Solution	Liposome	Liposome	Liposome
	LC_{50} (mM)		IG_{50} (mM)		LC_{50} (mM)	IG_{50} (mM)
NTI	0.08	0.08	0.02	0.02	0.16	0.015
α-MEI		>1.0		0.13	>1.0	0.12
MMI	1.5	>1.0	0.15	0.12	>1.0	0.04
PMI	~ 10.0	>1.0	0.12	0.12	>1.0	0.12
SMI	~ 10.0	>1.0	0.12	0.12	>1.0	0.12
OMI	~ 10.0	>1.0	0.18	0.15	>1.0	0.08
LMI	2.0	1.0	0.15	0.13	>1.0	0.04
Plain[b]		>10.0		>10.0	>10.0	5.2

LC_{50} and IG_{50} values are expressed in total lipid concentration (mM).
[a] Studies with solutions to RAW cells were not performed.
[b] EPC/Cholesterol 1:1 liposome was used as negative control.

3.5. Cellular uptake of antisense facilitated by AAI

Liposomes were prepared using different imidazole lipids and other naturally occurring helper lipids to assess delivery efficiency by means of the antisense activity of S-ODN. Depending on the lipid composition, each preparation showed differences in size distribution and S-ODN entrapment. In general, liposomes composed of AAI/EPC/DOPE entrapped more S-ODN than those composed of AAI/EPC/cholesterol. Further, liposomes containing saturated AAI (e.g. MMI and SMI) entrapped more S-ODN than those containing unsaturated AAI (i.e. OMI and LMI, data not shown).

The results of the functional assay were difficult to interpret: inhibition of luciferase expression in CV-1 cells by antisense activity of S-ODN delivered by AAI varied from one experiment to another. However, in a series of experiments, certain trends in structure–activity were observed (Table 4).

3.6. Intracellular distribution of F-ODN

When F-ODN (0.2 μM) alone was incubated with CV-1 cells in serum-free medium at 37 °C for 4 h, they were poorly internalized and only weak punctate fluorescence was observed in cytosol (Fig. 5A). In the presence of 10% whole FBS, punctate fluorescence was further attenuated (Fig. 5B). Liposomes composed of NTI/EPC/DOPE (1:5:4) contained 0.7 μM of F-ODN in a 5 mM total lipid concentration preparation. Upon fourfold dilution of this liposome preparation in serum-free medium, the total amount of NTI present in the culture medium was 0.125 mM. At this concentration, NTI appeared non-cytotoxic to CV-1 cells over the 4-h incubation. In this case, bright, punctate fluorescence was found in the cytosolic regions surrounding the nuclei (Fig.

Table 4
Effect of mole percentage of SMI in liposomes on antisense activity[a]

Lipid composition	SMI (%)	Cell viability (%)	Inhibition (%)
SMI/EPC/cholesterol 1:5:4	10	97	21
SMI/EPC/cholesterol 1:2:2	20	86	24
SMI/EPC/cholesterol 2:2:1[b]	40	74	45
SMI/EPC/DOPE 1:5:4	10	87	30
SMI/EPC/DOPE 1:2:2	20	67	51

[a] Single determination in CV-1 cells using an antisense luciferase down-regulation assay in CV-1 cells.
[b] Unstable liposomal formulation.

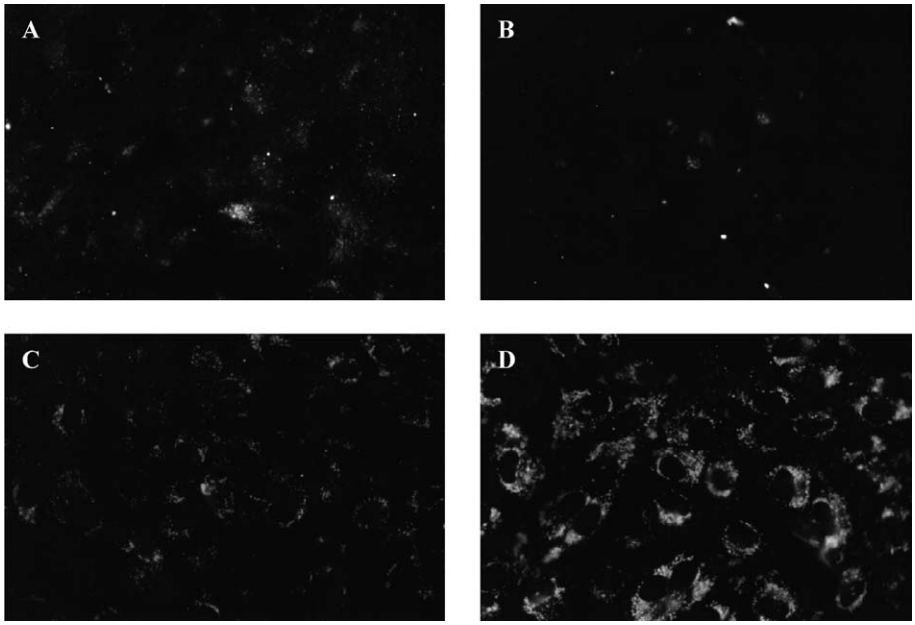

Fig. 5. Cellular uptake of F-ODN by CV-1 cells. F-ODN (0.2 μM) was fed to cells alone in serum-free medium (A) or in the presence of 10% FBS (B). F-ODN was also encapsulated in NTI/EPC/DOPE (1:5:4) liposomes (5 mM total lipid) and given to the cells after a fourfold dilution in serum-free medium (C) or in the presence of 10% FBS (D). After 4-h incubation at 37 °C, cells were fixed and examined by fluorescence microscopy.

5C and D). However, no fluorescence was detected inside the nuclei or the cytosol as a diffusive pattern.

The effect of 0%, 1%, 10%, or 20% SMI in 1:1 EPC/DOPE liposomes on the intracellular distribution of F-ODN is shown in Fig. 6. The average F-ODN concentration of the four liposome preparations was 1.51 ± 0.14 μM and the entrapment efficiency was approximately 30% at 5 mM total lipid concentration. Liposomal preparations were incubated with cells at 37 °C for 4 h after being diluted four times in serum-free medium. No cytotoxicity was observed during the period of experiment. In the presence of 0% or 1% SMI in liposomes, CV-1 cells showed similar punctate fluorescence (Fig. 6A and B) as that observed with F-ODN entrapped in NTI-containing liposomes. However, in the presence of 10% or 20% SMI in the liposomes, CV-1 cells showed not only bright punctate fluorescence in perinuclear

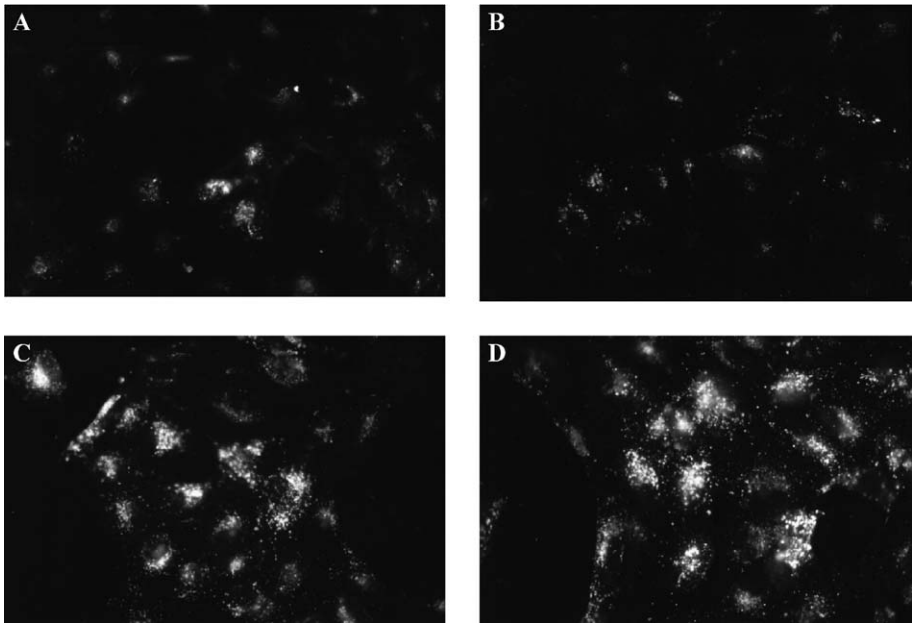

Fig. 6. Cellular uptake of liposomal F-ODN by CV-1 cells. F-ODN (1.5 μM) was encapsulated in SMI/EPC/DOPE liposomes (5 mM total lipid) containing (A) 0%, (B) 1%, (C) 10%, (D) 20 % of SMI. The liposome preparations were diluted fourfold in serum-free medium and given to cells. After 4-h incubation at 37 °C, cells were fixed and examined by fluorescence microscopy.

region but also a faint but significant diffuse fluorescence in some of the cells (Fig. 6C and D).

4. Discussion

The membrane-bound pK_a of AAI was not significantly affected by structural variations in the fatty acid chain: they were approximately the same (5.16 ± 0.03). The pK_a of α-MEI is about 0.13 units higher than the average pK_a of AAI mainly due to the slight electron donating effect of the methyl group at the α position. The pK_a values of all AAI are, however, significantly lower (1.0–1.2 unit) than that of tertiary amine NTI, due to the electron withdrawing effect of the ester bond next to the imidazole nitrogen. Most importantly, these results demonstrate that it is feasible to obtain cationic surfactants of desired pK_a through judicious chemical modifications near the polar head group. From the pK_a of the lipophilic weak bases listed in Table 1, a very broad spectrum of pK_a can be obtained by further selecting different weak base moieties for the polar head group of the molecule.

The pH-dependent surface activity of AAI was demonstrated by the pH-dependent aqueous solubility, micelle formation, and erythrocyte hemolysis. In the latter, the presence of various lag times implies a requirement of minimum threshold amount of MMI that must be accumulated in the plasma membrane of erythrocytes for hemoglobin leakage. As there were more surface-active protonated MMI present at a lower pH, less time was required to saturate the membrane. However, it should be noted that the neutral species of MMI is intrinsically active in disturbing the erythrocyte membranes, since complete hemolysis at a neutral pH still achieved in about 50 min. When superimposed upon the titration curve of MMI, the equivalent hemolysis rate–pH profile in Fig. 3B confirms the correlation between the rate of hemolysis by MMI and the amount of the surface-active protonated MMI. This observation suggests that one can control the rate of hemolysis or, in a more general term, membrane permeabilization, by adjusting the pK_a of the pH-sensitive detergents.

The stability study supports that incorporation of an ester moiety in AAI results in greater biochemical lability than their tertiary amine analog NTI. While we have not identified specific enzymes in either serum or cell homogenate responsible for hydrolysis of the ester bond, the first-order kinetics implies that under the experiment conditions, the esterase(s) was not saturated with the imidazole derivatives. A linear relationship was observed between k_S and log P, and also between k_H and log P (data not shown), for the three fully saturated AAI. This observation is consistent with a notion that in both cases it is the free, not protein-bound, AAI in human serum or CHO cell homogenate samples that dictated their rate of decomposition and that the intrinsic enzymatic activities toward all AAI are approximately the same. Hence, parameters such as aqueous solubility, protein binding, and self-association that determine the free AAI concentration in biological fluids are likely the key elements determining their overall susceptibility to enzymatic hydrolysis [26–28]. The higher lability of C18 unsaturated OMI and LMI in serum and cell homogenate suggests that other degradation mechanisms, in addition to the hydrolysis of the ester bond, may be responsible for their disappearance, e.g., oxidation of the double bonds. Finally, the serum stability of α-MEI is attributed to steric hindrance by the α-methyl group to enzymatic attack.

The significant decrease in cytotoxicity of AAI, in comparison with *N*-alkylimidazoles, generally supports the "soft drugs" concept developed by Bodor on labile quaternary ammonium salts [20]. However, within the group of six AAI investigated here, the apparent stability–cytotoxicity relationship is opposite to what was expected. For example, LMI and MMI were most labile, yet they were also the most toxic to RAW cells, but not CHO cells. One possible explanation for such behavior is the increased uptake of neutral liposomes by the former [8]. Following uptake, the hydrophilicity of LMI and MMI in comparison with other AAI could result in a higher availability of free lipid within RAW cells, thus showing increased toxicity. In the case of *N*-alkylimidazoles, biochemical stability rather than increased solubility appears to dictate their activity in vitro.

Having established structure–physicochemical property relationships, we tested if AAI can mediate cytosolic delivery of antisense oligonucleotides. Both fluorescent microscopy and a functional assay were employed. The intracellular distribution of F-ODN studied by fluorescence microscopy can possibly explain the poor overall antisense activity observed in the functional assay. Bright punctate fluorescence found in the cytosolic regions (Figs. 5 and 6) must correspond to endocytic compartments [29]. The lack of nuclear fluorescence staining or a diffuse fluorescence in the cytosol suggested that no S-ODN was available to hybridize target mRNA either in the cytosol or in the nucleus.

Although the fluorescence intensity exhibited in the cells treated with NTI/EPC/DOPE (1:5:4) liposomes entrapping F-ODN was greatly enhanced by the presence of 10% whole FBS, which presumably facilitated complement-mediated phagocytosis, no detectable diffusive fluorescence was found in nuclei or the cytosol. However, in the presence of 10% or 20% SMI-containing liposomes, CV-1 cells showed not only a bright punctate pattern in the cytosolic regions surrounding the nuclei but also diffuse fluorescence in some cells (Fig. 6C and D). This observation implies that incorporation of higher amounts of SMI into liposomes does facilitate partial escape of F-ODN from endosomes and enter the cytosol. Such intracellular distribution of F-ODN seems to be somewhat consistent with some, but not all, of the results obtained from the antisense activity of S-ODN. Indeed, in agreement with the above results, a trend was observed in the functional assay. The higher the percentage of SMI incorporated into liposomes, the greater the inhibition of luciferase expression in CV-1 cells observed.

NTI should provide more protonated species than AAI at a given pH because of the higher pK_a of NTI. However, F-ODN entrapped in liposomes containing NTI showed only punctate fluorescence inside the cells in contrast to cells treated with liposomes containing SMI. With the data available at present, we cannot adequately explain why NTI shows less membrane-permeabilizing activity than SMI. Having a shorter alkyl chain, it is possible that NTI is of higher CMC, thus requiring a larger amount to disrupt both liposomal as well as endosomal membranes [30,31]. A corollary is that morpholine- or piperazine-based lipids with a higher pK_a and low CMC might permeabilize liposomal and endosomal bilayers more efficiently.

Based on studies related to surfactant-induced release of liposome contents [32,33], it is postulated that for AAI to effectively facilitate the cytosolic delivery of antisense oligonucleotides, a large amount of AAI needs to be accumulated in one single endocytic compartment to reach a critical phospholipid to surfactant ratio. In liposomal systems, this phospholipid-to-surfactant ratio has been shown to increase with the size of the entrapped molecules [34]. It is conceivable that the amount of AAI needed to reach this critical ratio for release of macromolecules might be unattainably high. In addition, the dilution of surfactants in the endosome/lysosome milieu presents another obstacle to reach the required concentration. An ideal surfactant must saturate the endosomal membrane at the lowest possible concentration to facilitate cytosolic delivery. This critical amount, which must be accumulated in a single membrane compartment, is limited by the potency of the surfactant to disrupt membranes, the extent of incorporation of such lipids in liposomal bilayers and the cellular endocytic activity.

5. Conclusion

We have prepared a series of imidazole lipids to test the hypothesis that a lysosomotropic detergent with pH-dependent activity can permeabilize the endosomal membrane and promote cytosolic delivery of macromolecules. Acyloxyalkylimidazoles, each with an approximate pK_a of 5.2, displayed pH-dependent surface activity in hemolysis experiments. In addition, the imidazole lipids were degradable in serum and cell homogenate and displayed reduced cytotoxicity in comparison with other lipids such as NTI. However, no supportive evidence for the cytosolic delivery of liposome-entrapped antisense phosphorothioate oligos was observed in either the functional assay or fluorescence microscopy studies. Based on previous studies of surfactant-induced release of liposomal contents, we postulate that a large amount of imidazole lipids must be accumulated in a single endocytic compartment for effective cytosolic delivery. Such can be achieved by optimization of liposomal formulations of AAI to contain higher amounts of detergent. Alternatively, more potent pH-sensitive detergents based on stronger bases such as morpholine or piperazine can be synthesized to mediate efficient cytosolic delivery of entrapped macromolecules.

Acknowledgements

We wish to thank Dr. C. Leamon for the luciferase-expressing cell line CV-1 and Dr. E. LeCluyse for help with fluorescence microscopy. We would also like to thank Dr. Yilin Zhang for his advice, and Megabios (currently Valentis Inc.) for research support.

References

[1] S.A. Brockman, R.F. Murphy, in: K.L. Audus, T.J. Raub (Eds.), Biological Barriers to Protein Delivery, Plenum, New York, 1993, pp. 51–70.
[2] D.C. Drummond, M. Zignani, J. Leroux, Prog. Lipid Res. 39 (2000) 409–460.
[3] A. Asokan, M.J. Cho, J. Pharm. Sci. 91 (2002) 903–913.
[4] I.M. Hafez, S. Ansell, P.R. Cullis, Biophys. J. 79 (2000) 1438–1446.
[5] V. Budker, V. Gurevich, J.E. Hagstrom, F. Bortzov, J.A. Wolff, Nat. Biotechnol. 14 (1996) 760–764.
[6] P.M. Brown, J.R. Silvius, Biochim. Biophys. Acta 1023 (1990) 341–351.
[7] C.R. Miller, B. Bondurant, S.D. McLean, K.A. McGovern, D.F. O'Brien, Biochemistry 37 (1998) 12875–12883.
[8] T.D. Heath, N.G. Lopez, D. Papahadjapoulos, Biochim. Biophys. Acta 820 (1985) 74–84.
[9] A. Chonn, P.R. Cullis, D.V. Devine, J. Immunol. 146 (1991) 4234–4241.
[10] P.R. Cullis, A. Chonn, S.C. Semple, Adv. Drug Deliv. Rev. 32 (1998) 3–17.
[11] D.K. Miller, E. Griffiths, J. Lenard, R.A. Firestone, J. Cell Biol. 97 (1983) 1841–1851.
[12] P.D. Wilson, R.A. Firestone, J. Leonard, J. Cell Biol. 104 (1987) 1223–1229.
[13] S. Foster, L. Scarlett, J.B. Lloyd, Biochim. Biophys. Acta 924 (1987) 452–457.
[14] Z.I. Cabantchik, J. Silfen, R.A. Firestone, M. Krugliak, E. Nissani, H. Ginsburg, Biochem. Pharmacol. 38 (1989) 1271–1277.
[15] M.J. Boyer, I. Horn, R.A. Firestone, D. Steele-Norwood, I.F. Tannock, Br. J. Cancer 67 (1993) 81–87.
[16] E. Liang, J.A. Hughes, Biochim. Biophys. Acta 1369 (1998) 39–50.
[17] S. Simoes, V. Slepushkin, N. Duzgunes, M.C. Pedroso de Lima, Biochim. Biophys. Acta 1515 (2001) 23–37.
[18] Y. Nagawa, S.L. Regen, J. Am. Chem. Soc. 114 (1992) 1668–1672.
[19] O.A. Senkovich, E.A. Chernitsky, Membr. Cell Biol. 11 (1998) 679–689.
[20] N. Bodor, J. Med. Chem. 23 (1980) 469–474.
[21] M.J. Hope, M.B. Bally, G. Webb, P.R. Cullis, Biochim. Biophys. Acta 812 (1985) 55–65.
[22] D.W. Fry, J.C. White, I.D. Goldman, Anal. Biochem. 90 (1978) 809–815.
[23] A.L. Bailey, P.R. Cullis, Biochemistry 33 (1994) 12573–12580.
[24] C. Leamon, et al., Unpublished results, 1996.
[25] J. Carmichael, W.G. DeGraff, A.F. Gazdar, J.D. Minna, J.B. Mitchell, Cancer Res. 47 (1987) 936–942.
[26] C.G. Jordan, J. Pharm. Sci. 87 (1998) 880–885.
[27] K. Nambu, H. Miyazaki, Y. Nakanishi, Y. Oh-e, Y. Matsunaga, M. Hashimoto, Biochem. Pharmacol. 36 (1987) 1715–1722.
[28] E.J.F. Demant, G.V. Richer, A.M. Kleinfeld, Biochem. J. 363 (2002) 809–815.

[29] O. Zelphati, F.C. Szoka Jr., Pharm. Res. 13 (1996) 1367–1372.
[30] A. de la Maza, J.L. Parra, Chem. Phys. Lipids 77 (1995) 79–87.
[31] A. de la Maza, J.L. Parra, Biochim. Biophys. Acta 1300 (1996) 125–134.
[32] M. Almgren, Biochim. Biophys. Acta 1508 (2000) 146–163.
[33] D. Lichtenberg, R.J. Robson, E.A. Dennis, Biochim. Biophys. Acta 737 (1983) 285–304.
[34] J. Ruiz, F.M. Goni, A. Alonso, Biochim. Biophys. Acta 937 (1988) 127–134.